LTE UE Energy Saving by Applying Carrier Aggregation in a HetNet Scenario

Lauridsen, Mads; Wang, Hua; Mogensen, Preben

Published in:
Vehicular Technology Conference (VTC Spring), 2013 IEEE 77th

DOI (link to publication from Publisher):
10.1109/VTCSpring.2013.6692626

Publication date:
2013

Document Version
Accepted author manuscript, peer reviewed version

LTE UE Energy Saving by Applying Carrier Aggregation in a HetNet Scenario

Mads Lauridsen, Hua Wang, and Preben Mogensen
Department of Electronic Systems, Aalborg University, Niels Jernes Vej 12, DK-9220 Aalborg Øst
ml@es.aau.dk, huw@es.aau.dk, pm@es.aau.dk

***Abstract*—In this work it is examined if downlink Carrier Aggregation (CA) can be used to save UE energy. A dual-receiver LTE release 10 UE is compared with a single-receiver LTE release 8 UE. The models are based on scaling of an existing LTE release 8 UE power model. The energy consumption of the UEs is examined in a Heterogeneous Network scenario consisting of macro and small cells. The unexpected conclusion is that CA UEs can save energy, compared to LTE release 8 UEs, if they, depending on cell load, experience a throughput gain of 20 %. However if the UE throughput is unaltered the energy consumption can increase up to 20 %.**

I. Introduction

Carrier Aggregation (CA) has been standardized in LTE release 10, and it entails that the CA UE can connect to more than one component carrier (CC) in the downlink. Previously research has shown that CA can be used to provide better coverage and average throughput if carefully adjusted, [1]. Unfortunately little attention has been paid to how the increasingly complex requirements, [2], to the UE transceiver potentially can increase the energy consumption. Neither has it been examined if operators can adjust their LTE network, using CA, to help the CA UEs save energy.

In previous work Wang et al. [3], discussed CA UE structures and estimated the current consumption based on RF components' data sheets, but the energy consumption was not evaluated in a realistic scenario. The energy consumption of CA capable UEs was discussed in the 3GPP, [4], [5], when CA was proposed, but there are no accurate evaluations of how CA will affect the UE energy consumption. Deactivating the Secondary Cell [6], i.e. the UE does not receive or transmit from that cell, was however standardized to save UE energy.

In this work a novel CA UE power consumption model is proposed and it is shown that CA can actually prolong UE battery life if the network is configured properly. This novel conclusion is based on a comparison of LTE release 8 and 10 UEs' energy consumption in a Heterogeneous Network (HetNet) scenario consisting of macrocells and small cells.

First we propose a CA UE power consumption model, and then we describe the considered HetNet scenario. By combining the statistics from the HetNet simulation with the UE model the energy consumption is calculated and discussed. Finally the paper is concluded with recommendations for network operators who utilize CA.

II. Downlink CA UE Power Model Design

To evaluate the energy consumption of downlink CA UEs a power model is required. Currently only Qualcomm has announced a CA chip set [7], but because it is not yet commercially available an empirical model cannot be established. Therefore a CA model is derived from the existing LTE release 8 (R8) power model in [8]. The block diagram of the R8 model is shown in Fig. 1. The model is defined in Eq. (1) using the parameters in Tables I and II. Descriptions of how the parameters were defined and measured are given in [8].

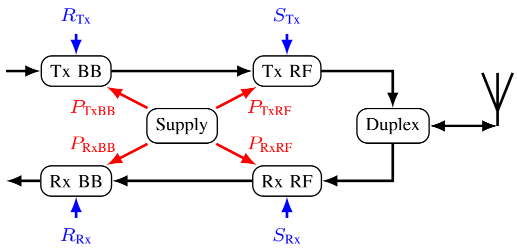

Fig. 1. LTE UE release 8 power model, [8, Fig.1]

TABLE I
First Order Polynomial Parameters, [8, Tab.3]

Part	Variable	p_0	p_1
Rx BB	R_{Rx} [Mbit/s]	-26.6 mW	2.89 mW/Mbit/s
Tx BB	R_{Tx} [Mbit/s]	34.5 mW	0.87 mW/Mbit/s
Rx RF	S_{Rx} [dBm]	-60.7 mW	-1.11 mW/dBm
Tx RF1[a]	S_{Tx} [dBm]	-71.3 mw	5.50 mW/dBm
Tx RF2[b]	S_{Tx} [dBm]	-943 mw	117 mW/dBm

[a] valid for $-30\,\text{dBm} \leq S_{Tx} \leq 10\,\text{dBm}$
[b] valid for $10\,\text{dBm} < S_{Tx} \leq 23\,\text{dBm}$.

TABLE II
Constant Parameters, [8, Tab.2].

Part	P_{idle}	P_{con}	P_{Rx}	P_{Tx}	P_{Rx+Tx}	P_{2CW}
Mode [-]	m_{idle}	$\overline{m_{idle}}$	m_{Rx}	m_{Tx}	$m_{Tx} \cdot m_{Rx}$	m_{2CW}
Value [W]	0.50	1.53	0.42	0.55	0.16	0.07

$$
\begin{aligned}
P_{tot} = & m_{idle} \cdot P_{idle} + \overline{m_{idle}} \cdot \{P_{con} + m_{Tx} \cdot m_{Rx} \cdot P_{Rx+tx} + \\
& m_{Rx} \cdot [P_{Rx} + P_{RxRF}(S_{Rx}) + P_{RxBB}(R_{Rx}) + m_{2CW} \cdot P_{2CW}] \\
& + m_{Tx} \cdot [P_{Tx} + P_{TxRF}(S_{Tx}) + P_{TxBB}(R_{Tx})]\} \quad [\text{W}] \quad (1)
\end{aligned}
$$

The four functions in Eq. (1) are evaluated using Table I and:

$$P_{part}\,(\text{variable}) = \text{variable} \cdot p_1 + p_0 \quad [\text{mW}] \qquad (2)$$

This work focuses on downlink CA and hence the transmitter part of the UEs is disabled in the following, i.e. $m_{Tx} = 0$. In 3GPP three band combinations have been defined, [9]:

1) Intra-band with contiguous component carriers (CCs)
2) Intra-band with non-contiguous CCs
3) Inter-band with non-contiguous CCs

together with two Release 10 UE receiver architectures [9]

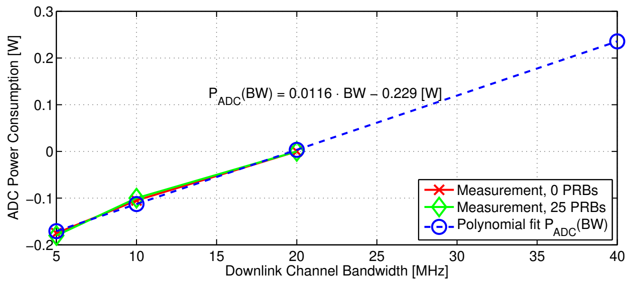

Fig. 2. ADC power consumption as a function of channel BW.

(a) Single Radio Frequency (RF) front-end with single wideband Analog-to-Digital Converter (ADC) and dual base band (BB) processor
(b) Dual RF with dual narrowband ADCs and dual BBs

Architecture (a) is only applicable in scenario 1, because it cannot filter undesired frequency content between non-contiguous CCs. Architecture (a) is however of interest because the hardware is less complicated and because scenario 1 will be used by some operators.

The R8 model was made for a 20 MHz downlink channel, but measurements were also performed for 5 and 10 MHz channels as shown in Fig. 2. The measurements were made using the Downlink Fixed MAC Padding for 0 and 25 DL PRBs, see [8] for further information. Based on those measurements a linear function of channel bandwidth is implemented in the R8 model and the receiver's power consumption is:

$$\begin{aligned} P_{\text{Rx, R8}} = & P_{\text{Rx}} + P_{\text{RxRF}}(S_{\text{Rx}}) + P_{\text{RxBB}}(R_{\text{Rx}}) \\ & + P_{\text{ADC}}(\text{BW}) + q_{\text{2CW, R8}} \cdot P_{\text{2CW}} \quad [\text{W}] \end{aligned} \tag{3}$$

The probability of using 2 codewords is q_{2CW}, and calculated by the simulator. Architecture (a), called release 10 wideband (R10wb), is defined as

$$\begin{aligned} P_{\text{Rx, R10wb}} = & P_{\text{Rx}} + P_{\text{RxRF}}(S_{\text{Rx}}) + P_{\text{ADC}}(\text{BW}) \\ & + [q_{\text{2CW, cc1}} + q_{\text{2CW, cc2}}] \cdot P_{\text{2CW}} \\ & + P_{\text{RxBB1}}(R_{\text{Rx1}}) + P_{\text{RxBB2}}(R_{\text{Rx2}}) \quad [\text{W}] \end{aligned} \tag{4}$$

and (b), called release 10 narrowband (R10nb), is defined as:

$$\begin{aligned} P_{\text{Rx, R10nb}} = & \, 2 \cdot P_{\text{Rx}} + P_{\text{RxRF1}}(S_{\text{Rx1}}) + P_{\text{RxRF2}}(S_{\text{Rx2}}) \\ & + P_{\text{RxBB1}}(R_{\text{Rx1}}) + P_{\text{RxBB2}}(R_{\text{Rx2}}) + P_{\text{ADC1}}(\text{BW1}) \\ & + P_{\text{ADC2}}(\text{BW2}) + [q_{\text{2CW, cc1}} + q_{\text{2CW, cc2}}] \cdot P_{\text{2CW}} \quad [\text{W}] \end{aligned} \tag{5}$$

The receivers' linear power functions are given in Table I and the ADC function is shown in Fig. 2. The ADC of rel10wb can handle two contiguous 20 MHz bandwidths while the rel8 and rel10nb are limited to 20 MHz per ADC.

The proposed CA power models are scaled versions of the published R8 model, because we believe the linear scaling is currently the best estimation available. The models do not include DRX [10] or micro-sleep, which is a method where a connected, but unscheduled UE can sleep during parts of a subframe [11], because the R8 model also does not include the methods. The idle mode power consumption P_{idle}, given in Table II, is therefore used as the UEs optimal low power mode. We anticipate DRX and micro-sleep will be of benefit in CA, because both receivers will not always be active.

The simulations are made such that when UE i has finished receiving the payload it will sleep for (using P_{idle} Watts)

$$t_{\text{sleep},i} = \max_{j\in[1,N]} (t_{\text{rx},j}) - t_{\text{rx},i} \qquad [\text{s}] \tag{6}$$

where $t_{\text{rx},j}$ is the receive time for UE j and N is the total number of UEs. The purpose is to compare all UEs over the same period of time as shown in Fig. 3. For later reference note that $t_{\max} = \max_{j\in[1,N]} (t_{\text{rx},j})$.

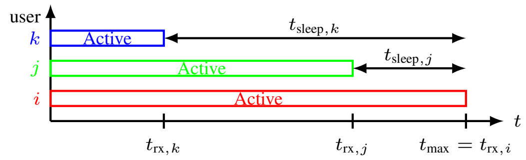

Fig. 3. Active and sleep time example for UEs i, j, and k.

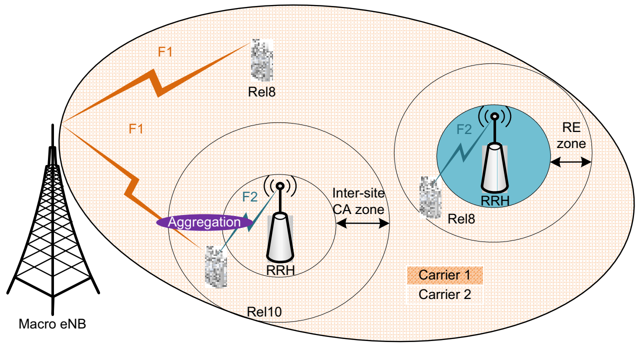

Fig. 4. Considered HetNet scenario with dedicated carrier deployment.

III. THE HETNET SCENARIO

HetNets are expected to be the next big leap in cellular system performance improvement by changing the topology of traditional networks which will bring the network closer to end users. In a HetNet, a mixture of macrocells combined with low-power nodes such as picocells, femtocells, and remote radio heads (RRHs) are used. The placement of macrocells is generally based on careful network planning to maximize the wide area coverage and control the inter-cell interference, while low-power nodes are deployed to either eliminate coverage holes in the macrocell or improve capacity at hotspot areas. In this paper, we focus on dedicated carrier deployment. Two contiguous CCs, each with 10 MHz bandwidth, are configured. One carrier frequency (CC1) is allocated to macro eNB whereas the other one (CC2) is allocated to small cells. The small cells are implemented as RRHs and are connected to macro eNBs via high bandwidth, low latency fibers. Thus, all baseband signal processing for the small cells (RRHs) could be placed in the macro eNB, allowing the aggregation of CCs between the macrocell (configured as primary serving cell (PCell)) and the small cell (configured as secondary serving cell (SCell)). Referring to the 3GPP terminology, the dedicated carrier deployment with macro and RRHs is denoted CA scenario 4 [6]. The R8 UEs can only connect to either the macro eNB or the RRH on the corresponding CC, based on downlink signal strength and the range expansion (RE) offset which is used to increase the footprint of small cells by adding a positive bias to the signal strength of low-power nodes during cell association [12]. The R10 UEs configured to operate with

CA can connect to both the macro eNB and the RRH using CA so that they can benefit from larger transmission bandwidth, and therefore opportunities to be served at higher data rates. The corresponding example of the considered deployment scenario is presented in Fig. 4.

It is worth mentioning that as the packet scheduler for the small cells (RRH) is physically located in the macro eNB, joint multicell packet scheduling [13] for those UEs configured with CA is feasible. The difference between independent and joint proportional fair (PF) scheduler lies in the calculation of the scheduling metric. In joint PF scheduler, the denominator of the PF metric is updated as the sum of the average scheduled throughput over all cells where the UE has been scheduled in the past. It simply requires information exchange on the average scheduled throughput between the scheduler for macro and small cells. In that way, the scheduler can essentially offer fast and efficient load balancing between macro and small cells, thereby allowing for more equitable distribution of radio resources among UEs. The comparisons between independent and joint PF scheduling across multiple CCs can be referred to [13] in the context of CA.

IV. Simulation Assumptions and Energy Consumption Results

The performance of the considered HetNet deployment scenarios is evaluated in a quasi-static downlink multi-cell system-level simulator that follows the LTE specifications, including detailed modeling of major radio resource management (RRM) functionalities. The network topology consists of 7 hexagonal macrocells transmitting at 40W with 3 sectors per cell. 4 RRHs transmitting at 1W are randomly placed within each sector. 2×2 MIMO with rank adaptation and interference rejection combining is configured. A bursty traffic model is considered where the call arrival follows a homogeneous Poisson process with fixed payload size per call. The average offered load per macrocell area is calculated as the product of the user arrival rate and the payload size. We assume hotspot UE distribution, where 2/3 of the UEs are dropped within a 40 m radius of the small cells while the remaining UEs are uniformly distributed within the macrocell area. The results in this section are for an offered cell load (OCL) of 10 Mbps and a UE payload of 10 Mb. Simulations were also performed with 20 Mb payload, but they do not affect the overall conclusions, and therefore the results are omitted. The scheduling granularity is 1 PRB. The UEs are mainly located around the small cells, and therefore the path gain to the small cell is lower as compared to the macrocell as shown in Fig. 5. For R10 UEs, it is assumed that they are always connected to both the macro and the most dominant RRH so that they can benefit from potential larger transmission bandwidth and fast inter-cell load balancing. This however does not entail that R10 UEs will always be scheduled on both CCs, as the scheduling of each CC is based on the channel quality and the cell load. For R8 UEs, different RE offsets are simulated. Only the optimal RE offset that maximizes the cell edge (5-percentile) throughput is used (RE=1.5dB with RSRQ cell selection for 10 Mbps OCL). Note R10 and R8 UEs are simulated separately.

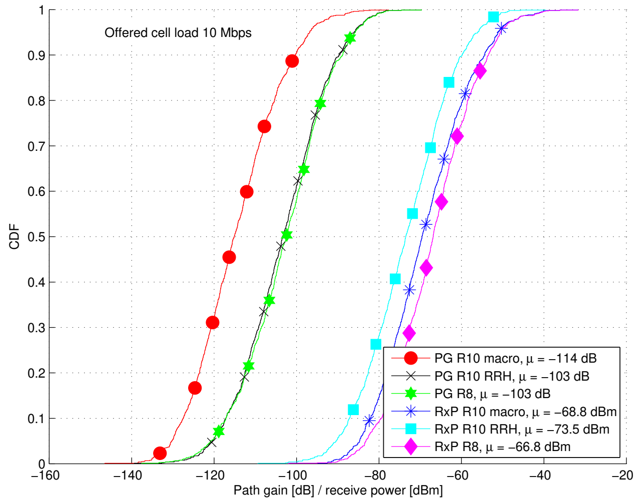

Fig. 5. Path gain (PG) & receive power (RxP). OCL=10 Mbps, μ is the mean.

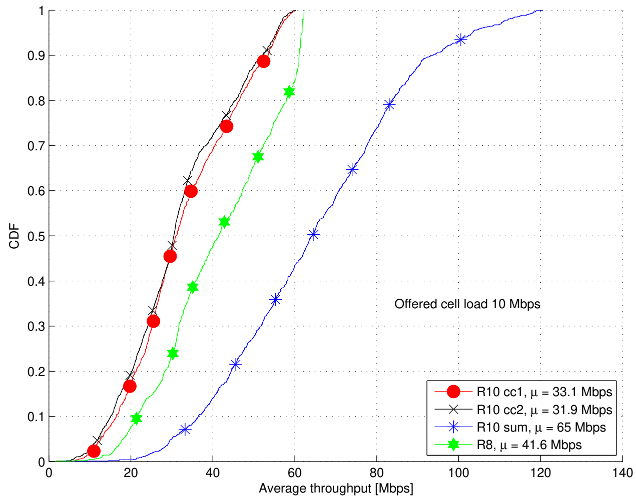

Fig. 6. Throughput. OCL = 10 Mbps, μ is the mean.

Fig. 6 shows the UEs' average throughput. The CA UEs achieve similar throughput on both CCs and $\sim$56 % higher throughput than the R8 UEs. This is due to the CA UE on average is allocated 95 PRBs while the R8 UE gets 48 PRBs. The CA UEs' higher throughput entail they receive the payload faster hence they can be in sleep mode for a longer duration.

The power consumption for each of the architectures is shown in Fig. 7. The R10nb on average uses 20 % more power than the R8 because the CA UE utilizes two receivers. Fig. 8 shows the total energy consumption of the UEs. The R10wb is the most energy efficient solution and on average 4 % can be saved, while the R10nb entails a saving of 3 %. The savings may not seem impressive, but it is of interest that CA does not introduce an energy consumption penalty on the UE given the model and scenario assumptions. The figure also contains a breakdown of the energy consumption in active and sleep mode. The R8 UE consumes more than 25 % extra energy in active mode compared to the CA UEs even though the actual power consumption of the R8 UE is 20 % lower as shown in Fig. 7. This is due to the lower throughput which entails the

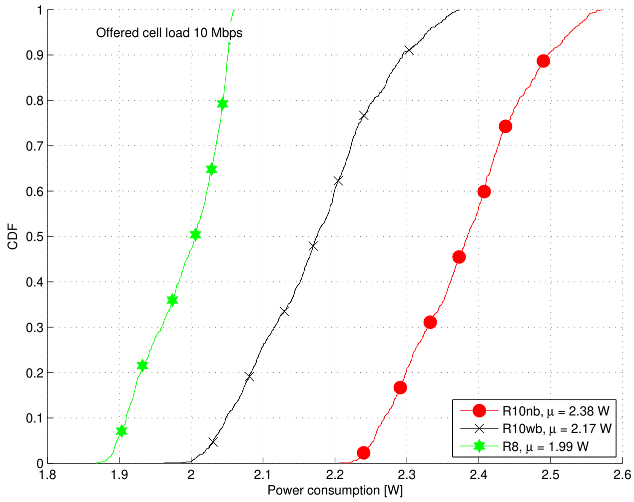

Fig. 7. Power consumption. OCL = 10 Mbps, μ is the mean.

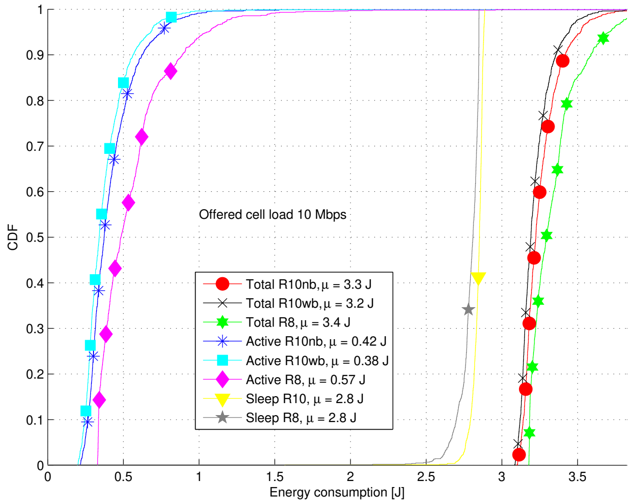

Fig. 8. Energy consumption. OCL = 10 Mbps, μ is the mean.

TABLE III
MEAN DATA RATE AND RECEIVE POWER.

Load [Mbps]	R_{R8} [Mbps]	$R_{R10\ cc1}$ [Mbps]	$R_{R10\ cc2}$ [Mbps]	$R_{R10\ sum}$ [Mbps]	S_{R8} [dBm]	$S_{R10\ cc1}$ [dBm]	$S_{R10\ cc2}$ [dBm]
10	42	33	32	65	−71	−69	−73
30	32	22	24	45	−72	−70	−73
50	24	15	17	31	−73	−72	−74
70	18	10	11	21	−74	−73	−75

UE has to remain active for a longer time in order to receive the same amount of data.

Given the major difference in active mode energy consumption major overall savings could be expected, but due to the sleep mode definition in Eq. (6) the UEs on average spend less than 10 % of the total time in active mode, hence the sleep mode energy consumption is dominant. The reason is that a single UE with low throughput prolongs the sleep time via t_{max}.

The simulations were also performed for other cell loads, and the mean values of these results are shown in the following Tables. Table III contains the results for mean throughput rate R and receive power S as a function of the cell load. The CA throughput gain decreases as the cell load increases because each UE is allocated less PRBs less often. Table

TABLE IV
MEAN RECEIVE TIME AND ENERGY CONSUMPTION.

Load [Mbps]	t_{R8} [s]	t_{R10} [s]	t_{max} [s]	$\frac{t_{R8}-t_{R10}}{t_{R8}}$ %	$\frac{t_{max}}{t_{R10}}$	E_{R8} [J]	E_{R10nb} [J]	E_{R10wb} [J]	$\frac{E_{R8}-E_{R10nb}}{E_{R8}}$ %
10	0.29	0.18	5.9	38	33	3.4	3.3	3.2	3
30	0.4	0.27	6.3	33	23	3.7	3.6	3.5	3
50	0.61	0.42	7	30	16	4.3	4.2	4.1	3
70	0.96	0.68	9.2	29	13	5.9	5.7	5.6	3

TABLE V
MEAN VALUES USING A MINIMUM THROUGHPUT LIMIT OF 5 MBPS.

Load [Mbps]	t_{R8} [s]	t_{R10} [s]	t_{max} [s]	$\frac{t_{R8}-t_{R10}}{t_{R8}}$ %	$\frac{t_{max}}{t_{R10}}$	E_{R8} [J]	E_{R10nb} [J]	E_{R10wb} [J]	$\frac{E_{R8}-E_{R10nb}}{E_{R8}}$ %
10	0.28	0.18	1.6	37	9	1.2	1.1	1.1	7
30	0.39	0.27	2	32	7	1.5	1.5	1.4	6
50	0.56	0.42	2	25	5	1.8	1.7	1.6	3
70	0.76	0.65	2	15	3	2	2.1	2	−2

IV contains the associated results for mean receive time t and energy consumption E. The first thing to observe is that the receive time difference between R8 and R10 decreases as the cell load increases. Furthermore the ratio between the longest receive time and average R10 receive time decreases as the load increases because the average throughput approaches the minimum throughput i.e. the throughput spread is much smaller, when the cell load is high. This means the sleep time is very significant for all loads hence the sleep energy is the major contributor to the total energy consumption. The relative energy consumption difference between R8 and R10 is almost constant. The reasons are that the active time ratio is almost constant and that the sleep mode, which consumes the same amount of energy for both releases, is dominating.

Due to the sleep time definition in Eq. (6) a slowly downloading UE will entail all other UEs experience long sleep times. In the previous results this meant the sleep energy was dominating and therefore an artificial simulation campaign was made, where UEs with a throughput below 5 Mbps were excluded from the statistics. This results in a lower maximum receive time as shown in Table V. The 5 Mbps throughput limit affects all scenarios, and it is clear that CA has an advantage in low cell load scenarios where the energy savings now are 5-7 %. When the cell load is increased the difference between R8 and R10 receive times decreases. This means the active energy consumption of the R8 UE becomes smaller than the CA UE hence the CA energy advantage is lost.

As discussed in section II CA can obtain even higher energy savings by the use of DRX and/or micro-sleep, because the CA UE is scheduled less often when it is in RRC_connected mode. Fig. 9 shows the UE activity factor, which is the ratio between scheduled time and connected mode time, of the simulated 70 Mbps cell load scenario. When the UE is connected to the macrocell it is scheduled less than 50 % of the time, and based on the assumptions in [11], where it is estimated that the energy consumption in micro-sleep mode is half of the active mode, the energy consumption can be reduced by ∼25 %. One reason for the low activity factor is due to the CA UE always being connected to both CCs even though one of the CCs may experience so low path gain that it cannot serve the UE.

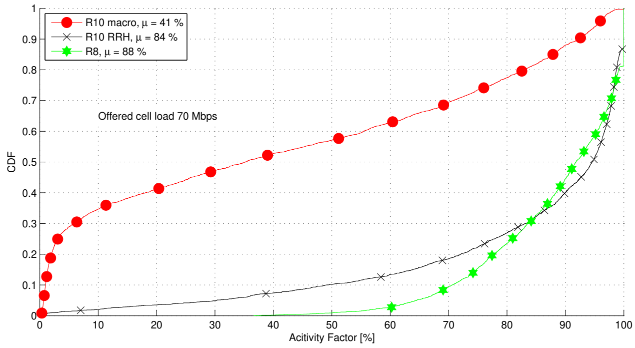

Fig. 9. Activity Factor. OCL = 70 Mbps, μ is the mean.

TABLE VI
MEAN POWER VALUES AND BREAK-EVEN POINTS FOR 10 MB PAYLOAD.

Load [Mbps]	P_{R8} [W]	P_{R10nb} [W]	P_{R10wb} [W]	$1-x_{nb}$ %	$1-x_{wb}$ %
10	2	2.4	2.2	21	11
30	2	2.3	2.1	19	9
50	1.9	2.3	2	19	8
70	1.9	2.2	2	19	7

V. ENERGY BREAK-EVEN

The results in the previous section showed that CA can be used to save UE energy. The savings are possible when the UE, using CA, receives a certain file faster than it would have without CA. In this section the break-even point i.e. the required increase in throughput to make CA energy efficient, is calculated. The energy consumed by a R8 UE is:

$$E_{R8} = P_{R8} \cdot t_{rx} + P_{sleep} \cdot (t_{\max} - t_{rx}) \quad [\mathrm{J}] \tag{7}$$

The receive time t_{rx} is scaled by x so the CA UE consumes

$$E_{R10} = P_{R10} \cdot t_{rx} \cdot x + P_{sleep} \cdot (t_{\max} - t_{rx} \cdot x) \quad [\mathrm{J}] \tag{8}$$

The break-even point i.e. the scaling factor x is

$$E_{R8} = E_{R10} \quad [\mathrm{J}]$$
$$P_{R8} \cdot t_{rx} - P_{sleep} \cdot t_{rx} = P_{R10} \cdot t_{rx} \cdot x - P_{sleep} \cdot t_{rx} \cdot x \quad [\mathrm{J}]$$
$$x = \frac{P_{R8} - P_{sleep}}{P_{R10} - P_{sleep}} \quad [-] \tag{9}$$

The break-even point is calculated for the simulated cell loads and shown in Table VI. The sleep power is 0.50 W for all UEs. The power consumption decreases as the load increases because the UE throughput also decreases meaning that the baseband processor is less loaded. When the R10nb is applied a throughput increase of 19-21 % is required to break even. If the R10wb is used the increase shall be as little as 7-11 %. The conclusion that the throughput must be increased in order to enter sleep mode fast and save energy e.g. by scheduling one UE continuously is similar to the conclusion that was reached for uplink transmission in [14]. Therefore it is expected that the same conclusion can also be applied to uplink CA.

VI. CONCLUSION

Carrier Aggregation (CA) is standardized in LTE release 10 to improve throughput and coverage. However this entails a more complicated transceiver design, hence a potential increase in UE energy consumption. In this study it was shown that CA can actually be used to save UE energy if the downlink throughput is increased 20 %, hence this is what network operators should aim for.

In this work two CA UE architectures where mapped to a power model, and the energy consumption of the new UEs were compared with an existing LTE release 8 UE in a Heterogeneous Network scenario. The reason why energy can be saved is that the CA UE can enter sleep mode faster, and this low-power state is the key to save energy in current UE architectures. If the LTE network using CA is implemented to improve the coverage the throughput gain may be small. This can entail the CA UEs experience an increased energy consumption of up to 20 %. Discontinuous Reception and the micro-sleep concept can add to the CA's advantage because the CA UE is likely to be scheduled less often, when it is in connected mode and receiving finite buffer traffic.

To summarize CA can be used to increase the throughput, and moreover decrease UE energy consumption, both key performance indicators leading to a better user experience.

ACKNOWLEDGEMENT

Thanks to Nokia Siemens Networks Aalborg for providing comments and statistics. The work is partly funded by the Danish National Advanced Technology Foundation and the 4th Generation Mobile Communication and Test Platform project.

REFERENCES

[1] K. Pedersen, F. Frederiksen, C. Rosa, H. Nguyen, L. Garcia, and Y. Wang, "Carrier Aggregation for LTE-Advanced: Functionality and Performance Aspects," *Communications Magazine, IEEE*, vol. 49, no. 6, pp. 89 –95, june 2011.
[2] D. Bai, C. Park, J. Lee, H. Nguyen, J. Singh, A. Gupta, Z. Pi, T. Kim, C. Lim, M.-G. Kim, and I. Kang, "LTE-Advanced Modem Design: Challenges and Perspectives," *Communications Magazine, IEEE*, vol. 50, no. 2, pp. 178 –186, february 2012.
[3] Y. Wang, D. Xiao, and W. Wang, "A Research on Power Consumption of Receiver in CA Scenarios," in *Information Engineering (ICIE), 2010 WASE International Conference on*, vol. 1, aug. 2010, pp. 247 –250.
[4] Motorola, "Spectrum Aggregation Operations - UE Impact Considerations," 3GPP R1-084405, 2008.
[5] N. Docomo, "Views on Downlink Reception Bandwidth Considering Power Saving Effect in LTE-Advanced," 3GPP R1-090310, 2009.
[6] Z. Shen, A. Papasakellariou, J. Montojo, D. Gerstenberger, and F. Xu, "Overview of 3GPP LTE-Advanced Carrier Aggregation for 4G Wireless Communications," *Communications Magazine, IEEE*, vol. 50, no. 2, pp. 122 –130, February 2012.
[7] Qualcomm, "Qualcomm Third Generation LTE Chipsets are first to Support HSPA+ Release 10, LTE-Advanced with LTE Carrier Aggregation," http://www.qualcomm.com, 2012.
[8] A. Jensen, M. Lauridsen, P. Mogensen, T. Sorensen, and P. Jensen, "LTE UE Power Consumption Model - for System Level Energy and Performance Optimization," *VTC Fall 2012*, September 2012.
[9] 3GPP, "Feasibility Study for Further Advancements for E-UTRA (LTE-Advanced)," TS 36.912 V9.3.0, 2010.
[10] C. Bontu and E. Illidge, "Drx mechanism for power saving in lte," *Communications Magazine, IEEE*, vol. 47, no. 6, pp. 48 –55, june 2009.
[11] M. Lauridsen, A. Jensen, and P. Mogensen, "Fast Control Channel Decoding for LTE UE Power Saving," *VTC Spring 2012*, May 2012.
[12] K. Pedersen, Y. Wang, B. Soret, and F. Frederiksen, "eICIC Functionality and Performance for LTE HetNet Co-Channel Deployments," *VTC Fall 2012*, September 2012.
[13] Y. Wang, K. Pedersen, P. Mogensen, and T. Sorensen, "Carrier Load Balancing and Packet Scheduling for Multi-carrier Systems," *Wireless Communications, IEEE Transactions on*, vol. 9, pp. 1780 –1789, 2010.
[14] M. Lauridsen, A. Jensen, and P. Mogensen, "Reducing LTE Uplink Transmission Energy by Allocating Resources," in *VTC Fall*, Sep 2011.